Ferroelectrics

ISSN: (Print) (Online) Journal homepage: https://www.tandfonline.com/loi/gfer20

Phase structure, microstructure, and dielectric properties of (1–*x*)Pb($Zr_{0.50}$ $Ti_{0.50}$)O_3–*x*Ba($W_{2/3}$ $Mn_{1/3}$)O_3 ceramics

Fares Kahoul, Louanes Hamzioui, Abderrezak Guemache, Michel Aillerie & Ahmed Boutarfaia

To cite this article: Fares Kahoul, Louanes Hamzioui, Abderrezak Guemache, Michel Aillerie & Ahmed Boutarfaia (2021) Phase structure, microstructure, and dielectric properties of (1–*x*)Pb($Zr_{0.50}$ $Ti_{0.50}$)O_3–*x*Ba($W_{2/3}$ $Mn_{1/3}$)O_3 ceramics, Ferroelectrics, 572:1, 229-237, DOI: 10.1080/00150193.2020.1868885

To link to this article: https://doi.org/10.1080/00150193.2020.1868885

Published online: 09 Mar 2021.

FERROELECTRICS
2021, VOL. 572, 229–237
https://doi.org/10.1080/00150193.2020.1868885

Taylor & Francis
Taylor & Francis Group

Phase structure, microstructure, and dielectric properties of $(1-x)Pb(Zr_{0.50}\ Ti_{0.50})O_3-xBa(W_{2/3}\ Mn_{1/3})O_3$ ceramics

Fares Kahoul[a,b], Louanes Hamzioui[a,b], Abderrezak Guemache[a], Michel Aillerie[c,d], and Ahmed Boutarfaia[b]

[a]Département Socle Commun ST, Faculté de Technologie, Université de M'Sila, M'Sila, Algérie; [b]Université de Biskra, Département de Chimie, Laboratoire de Chimie Appliquée, RB-Biskra, Algérie; [c]Université de Lorraine, LMOPS, Metz, EA, France; [d]Centrale Supelec, LMOPS, Metz, France

ABSTRACT

Ceramics in (1-*x*)PZT–xBWM system with formula (1-*x*)$Pb(Zr_{0.50}\ Ti_{0.50})O_3$–*x*$Ba(W_{2/3}\ Mn_{1/3})O_3$, where $x = 0.0025$–0.01, were prepared by a normal solid-state method and sintered at 1150 °C. The crystal structure, microstructure and dielectric properties of the ceramics were investigated via X-ray diffraction, scanning electron microscopy and dielectric spectroscopy. X-ray diffraction results demonstrate that all the samples lie within the morphotropic phase boundary region. A microstructure with mean grains sizes of 1.71–2.11 μm were found and the apparent density of 7.59–7.75 g/cm^3. The Curie temperature (T_c) decreases with increasing BWM content. The room temperature dielectric constant shows a decreasing trend while loss improves with BWM doping.

ARTICLE HISTORY
Received 25 February 2020
Accepted 25 November 2020

KEYWORDS
Dielectric; XRD; solid-state reaction; scanning electron microscopy

1. Introduction

Lead zirconate–titanate ($PbZr_xTi_{1-x}O_3$) or PZT ceramics are a class of piezoelectric materials that are currently experiencing widespread use in industry as electromechanical devices. Compositions close to the morphotropic phase boundary (MPB) describe the area where the two ferroelectric modifications of PZT coexist and are of huge industrial interest [1, 2].

The study of MPB solid solutions is not only of scientific interest but also of technological importance in creating novel memory devices [3]. PZT solid solutions are commonly prepared by solid-state reactions [3]. Considerable research effort has been concentrated on the MPB and dielectric properties of PZT ceramics [4–6].

PZT compositions show significant merit when they are doped with foreign ions. Its dielectric and piezoelectric properties change, depending on the site occupied by the foreign ion in ABO_3 perovskite structure. Dopants are classified as isovalent, acceptors or donors [7]. Donors (trivalent ion at A site and pentavalent ion at B site) reduces the concentration of intrinsic oxygen vacancy created due to PbO evaporation and compensate the hole formed due to lead vacancies, which in turn increases bulk resistance of the sample. Acceptors (monovalent at A site and trivalent at B site) introduces oxygen

CONTACT Fares Kahoul Fares.kahoul@univ-msila.dz; Fares_260@yahoo.fr

vacancies to maintain charge neutrality, due to this oxygen vacancy domain walls gets pinned and space charges are introduces, which in turn reduces grain resistance and inhibits domain motion [8], also acceptor-doped PZT shows poor hysteresis loop and low dielectric constant. Isovalent (divalent at A site and tetravalent at B site) doping tends to reduce the Curie temperature [9] and increases the density of PZT ceramic, which in turn affects the electrical properties.

The overall purpose of this study is to determine the phase formation and dielectric properties of ceramics in a (1-x)Pb($Zr_{0.50}$ $Ti_{0.50}$)O_3–xBa($W_{2/3}$ $Mn_{1/3}$)O_3 (where $x = 0.0025$, 0.005, 0.0075, and 0.01) system prepared by the conventional solid-state process.

2. Experimental procedures

The compositions of (1-x)Pb($Zr_{0.50}$ $Ti_{0.50}$)O_3–xBa($W_{2/3}$ $Mn_{1/3}$)O_3 ((1-x)PZT–xBWM, where $x = 0.0025$, 0.005, 0.0075,and 0.01) were prepared by the conventional solid-state method. Commercially available PbO, ZrO_2, TiO_2, BaO, WO_3, and Mn_2O_3 oxide powders (with purity >99%) were used as the starting materials. All the powders were mixed and milled in ethanol as dispersion medium for 24 h and then calcined at 850 °C for 4 h. The calcined powders were reground and mixed with a binder of 5 wt% polyvinyl alcohol (PVA) solution and pressed into disks with 8 mm in diameter and about 1 mm in thickness. The green disks were heated at 650 °C for 3 h to eliminate PVA and finally sintered at 1150 °C for 3 h in air atmosphere. Both sides of the sintered ceramics were pasted with silver electrodes for measurement of the electrical properties.

Room temperature powder X-ray patterns were recorded on a Philips diffractometer using Cu K_α radiation with a wave-length of $\lambda_1 = 1.54056$ Å in the angle range of $20° \leq 2\theta \leq 70°$ with a 10 s counting time for each step of 0.02°. The density of the sintered ceramics was measured by the Archimedes method. The microstructure of the ceramics was examined by scanning electron microscopy (SEM). Dielectric measurements were performed on ceramic disks by an LCR meter HP4284A. The temperature and frequency ranged between 298 and 800 K and 1–20 kHz, respectively.

3. Results and discussion

3.1. Structural and microstructural properties

X-ray diffraction (XRD) patterns of (1-x)PZT–xBWM ceramics with various x values, measured at room temperature are shown in Fig. 1. All samples showed a complete crystalline solution of perovskite structure with the presence of pyrochlore.

It is known that the (200) pseudo cubic reflection is splitted into two peaks for the tetragonal (T) phase, whereas it is a singlet for a rhombohedral (R) phase, and while the triplet splitting of this reflection is an indication of the presence of both rhombohedral (R) and tetragonal (T) phases (MPB) in the system [5, 10–14]. The X-ray diffraction profiles of BWM added PZT systems in the range 42°–48° to examine the (200) reflection for MPB.

The X-ray diffraction profile for (1–x)PZT–xBWM ceramic indicated a coexistence region (MPB) comprising of two phases viz rhombohedral and tetragonal phases.

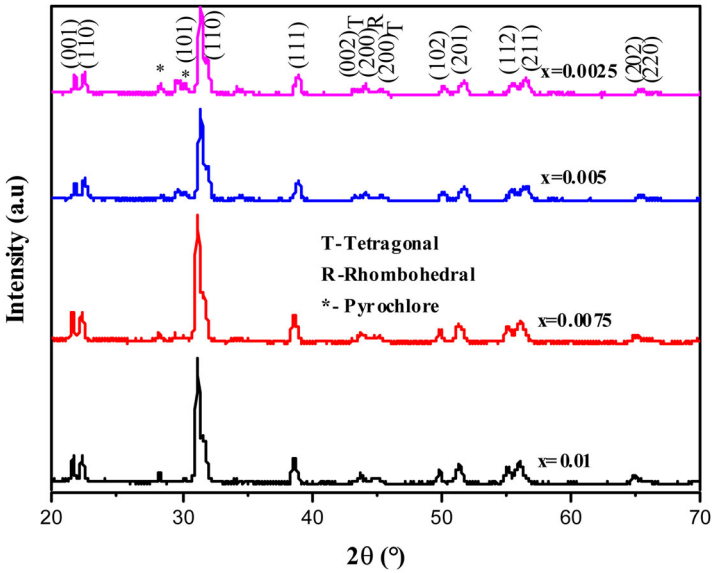

Figure 1. XRD diffraction patterns of (1–*x*)PZT–*x*BWM powders.

However, with the addition of BWM in the PZT system ($x = 0.0025$–0.01), the gradual transformation of the triplet splitting of the peaks into two peaks is observed, thus, indicating that the BWM addition favors the tetragonal phase in the system.

Therefore, the coexistence of tetragonal and rhombohedral phases occurs for the PZT–BWM ceramics at room temperature, demonstrating that the ceramics lie at the morphotropic phase boundary (MPB) [5, 15]. Because the peaks shift to higher angles, it is assumed that $(Ti,Zr)^{4+}$ is substituted by W^{6+} and Mn^{3+}, suggesting a change of the unit cell volume. This change may be due to the formation of complete solid solutions between the BWM content and the PZT–BWM ceramics, which leads to a distortion of the crystal lattice. The addition of the BWM solid solution promotes the substitution of the Pb^{2+} A and/or Zr^{4+}/Ti^{4+} B site of the perovskite structure more effectively than the addition of raw metal oxides, and then increases structure defects and decreases the barrier among domains. The formation of the BWM solid solution is beneficial to the diffusion of ions.

Figure 2 displays the average grain size and the density of (1-*x*)PZT–xBWM-based ceramics with different BWM contents ($x = 0.0025$, 0.005, 0.0075 and 0.01 mol %). The average grain size was calculated using the line-intercept method. The grain sizes start to increases with increasing x content from 1.71 μm ($x = 0.0025$) to 2.11 μm ($x = 0.01$). Conversely, the density of the ceramics decreases with increasing the x content.

This can be attributed to the fact that the x content facilitates grain growth by increasing the diffusion mobility resulting from the liquid phase or/and oxygen deficiency vacancies [12, 16]. Due to this oxygen vacancy domain walls get pinned and reduces grain size. Also, these oxides get precipitated at the grain boundary that subsequently resists the grain growth [5]. However, For $x = 0.0075$ and 0.01, a larger grains impact increases grain boundary mobility, and thus promotes grain growth, resulting in a reduction in the bulk density of ceramics [12].

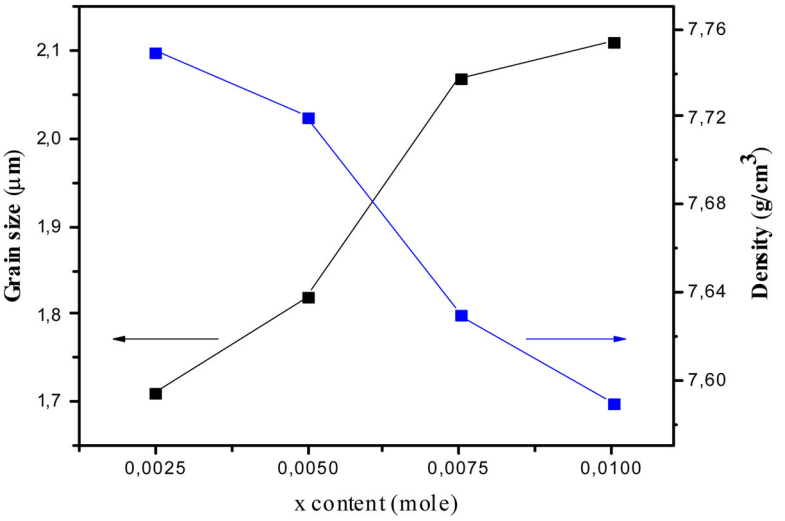

Figure 2. Variation of the grain size, and density as a function of *x* content.

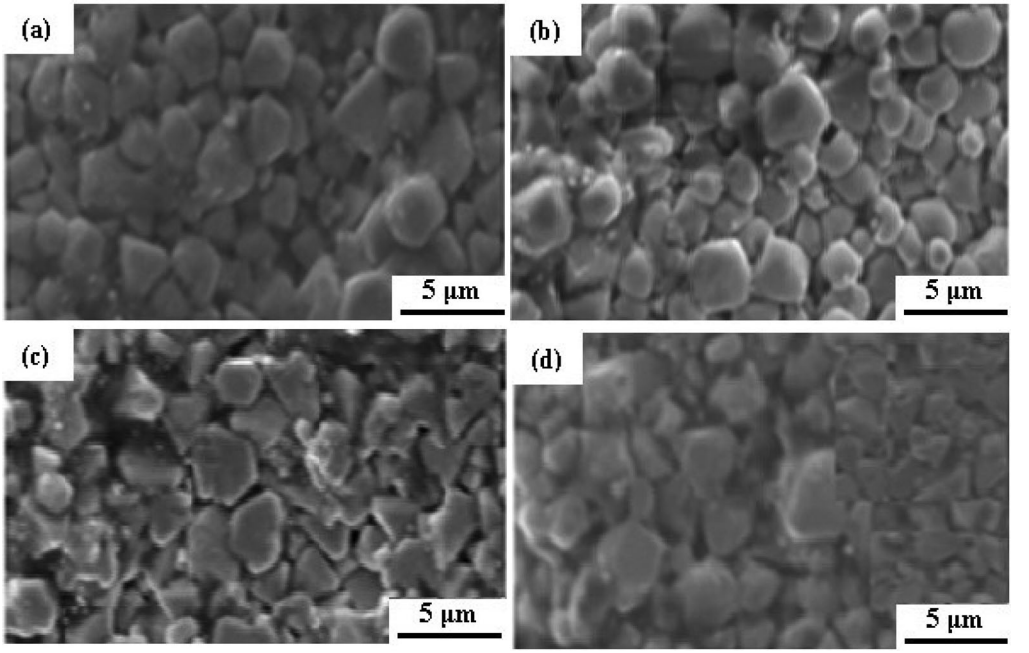

Figure 3. SEM micrographs of (1–*x*)PZT–*x*BWM with various compositions: (a) $x = 0.0025$, (b) $x = 0.005$, (c) $x = 0.0075$, and (d) $x = 0.01$.

Figure 3(a–d) shows the surface morphologies of (1-*x*)Pb($Zr_{0.50}$ $Ti_{0.50}$)O_3–xBa($W_{2/3}$ $Mn_{1/3}$)O_3 ceramics with $x = 0.0025$, 0.005, 0.0075 and 0.01, respectively. With the increase of BWM content, the (1–*x*)Pb($Zr_{0.50}$ $Ti_{0.50}$)O_3–*x*Ba($W_{2/3}$ $Mn_{1/3}$)O_3 ceramics become less dense, and their average grain size gradually increases (Fig. 2), and reveal

that the pores are free and the tightly bound grains promote densification in the ceramics. Thus, in the present study, BWM plays a significant role in defining the microstructural characteristics of PZT–BWM ceramics. In this system, the homogenization is caused by the greater atomic diffusion.

3.2. Dielectric properties

Dielectric measurement can give information about the electric properties of a material as a function of frequency and temperature. The analysis of dielectric property measures two electrical characteristics of the materials. One is capacitive which is related to the insulating nature of the materials and it represents the ability to store the charges and, second one is the conductive nature of the materials which gives the information about the electronic charge transport. Through this analysis, the dielectric constant (ε_r) and dielectric loss (tanδ) of a material can be determined which will explore the technological application [17].

The variation of dielectric constants ε_r of all the composite samples (1-x)Pb($Zr_{0.50}$ $Ti_{0.50}$)O_3–xBa($W_{2/3}$ $Mn_{1/3}$)O_3 for $x = 0.0025$, 0.005, 0.0075 and 0.01 with temperature (298–800 K) at different frequencies (1 kHz to 20 kHz) are shown in Fig. 4. For all the samples it is observed that ε_r decreases with an increase in frequency, which is a general feature of polar dielectric materials irrespective of the composition of the specimens. The higher values of ε_r at lower frequency are due to the simultaneous presence of all types of polarizations (space charge, dipolar, ionic, electronic, etc.) which is found to decrease with the increase in frequency [18–20]. The position of dielectric maxima does not change with frequency. This indicates characteristics of normal ferroelectrics [21, 22].

The value of ε_r increases gradually on increasing temperature to its maximum value (ε_{max}), and then decreases. This dielectric anomaly indicates a phase transition from ferroelectric to paraelectric phase at that particular temperature, usually called as Curie or transition temperature (T_c) [18, 20, 23].

The temperature dependence of dielectric loss (tanδ) at selected frequencies of (1–x)PZT–xBWM is shown in Fig. 5. It is observed that the dielectric loss increases with increasing temperature and decreases with increasing frequency [24]. The nature of variation of tanδ at higher frequency and temperature can be explained by space-charge polarization [19, 25].

It has been found that the dissipation factor (tanδ) is very low and is almost constant for all compositions at lower temperatures; however, above 673 K, a sharp increase in dielectric loss was observed. The increase in the loss at elevated temperatures is caused by a corresponding conductivity increase [26]. This may be due to the fact that a limited number of mobile ions in an ionic solid are trapped in relatively stable potential wells during their movement through the solids. Due to an increase in temperature, donor cations begin to play a major role in the conduction process. These donors create a level very close to the conduction band; a small amount of energy is needed to activate them.

The dielectric loss (tanδ) at room temperature decreases with increasing BWM content (upto $x = 0.005$) and then increases (data presented in Table 1), which is in line with the previous literature [27].

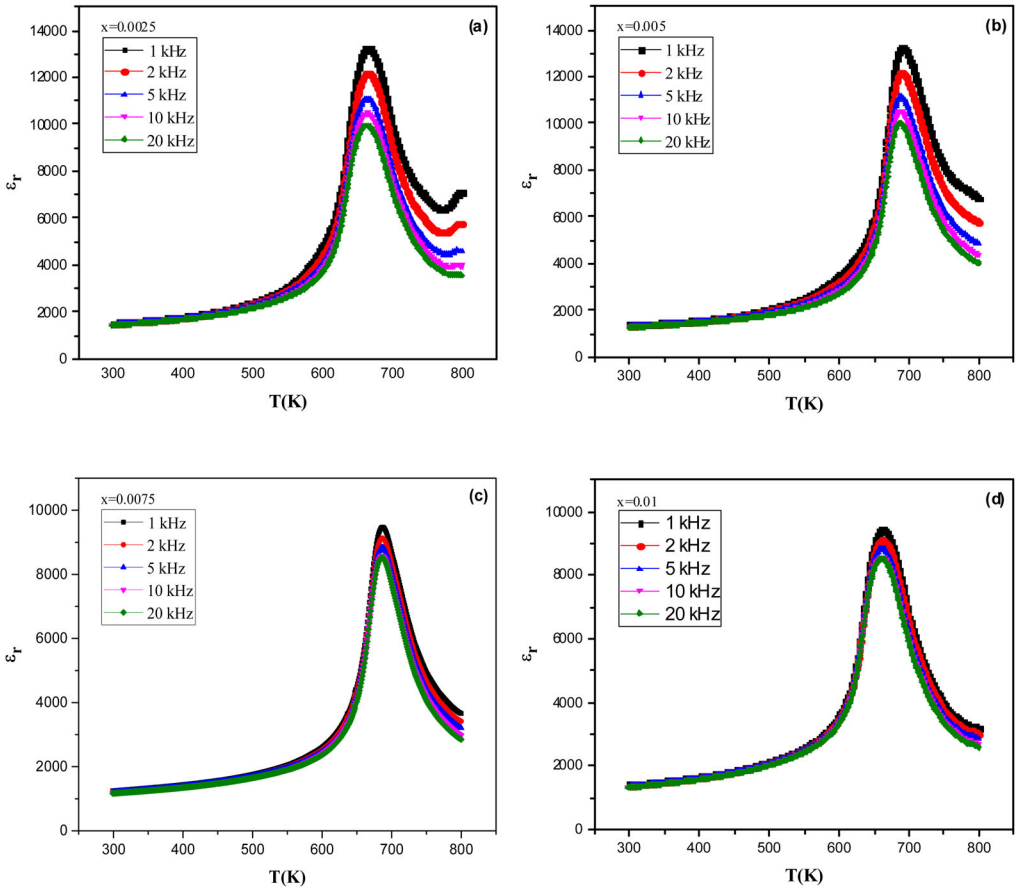

Figure 4. Temperature dependence of dielectric constant (ε_r) at different frequencies for $(1-x)Pb(Zr_{0.50}\ Ti_{0.50})O_3-xBa(W_{2/3}\ Mn_{1/3})O_3$ system: (a) $x = 0.0025$, (b) $x = 0.005$, (c) $x = 0.0075$, and (d) $x = 0.01$).

The dielectric properties at 1 kHz for the various studied systems are listed in Table 1. The Curie temperature significantly decreases with increasing BWM content that is due to the weakening of ferroelectric strength by BWM substitution. There is a significant decrease in dielectric constant at T_C with an increase in x. These results show that a large quantity of the two dopants (W, Mn) replaces the B site of the perovskite structure, thus reducing the resistance of the B-O bond and decreasing the Curie temperature of the specimens.

4. Conclusions

The dielectric properties of $(1-x)Pb(Zr_{0.50}\ Ti_{0.50})O_3-xBa(W_{2/3}\ Mn_{1/3})O_3$, where $x = 0.0025$, 0.005, 0.0075, and 0.01 ceramics formed via a normal solid-state method. Structural and dielectric properties of the materials have been studied. XRD analysis reveals the co-existence of tetragonal and rhombohedral (MPB) phases for all the samples. The SEM micrograph showed that the average grain size significantly increases with increasing BWM content. Detailed studies of dielectric properties of

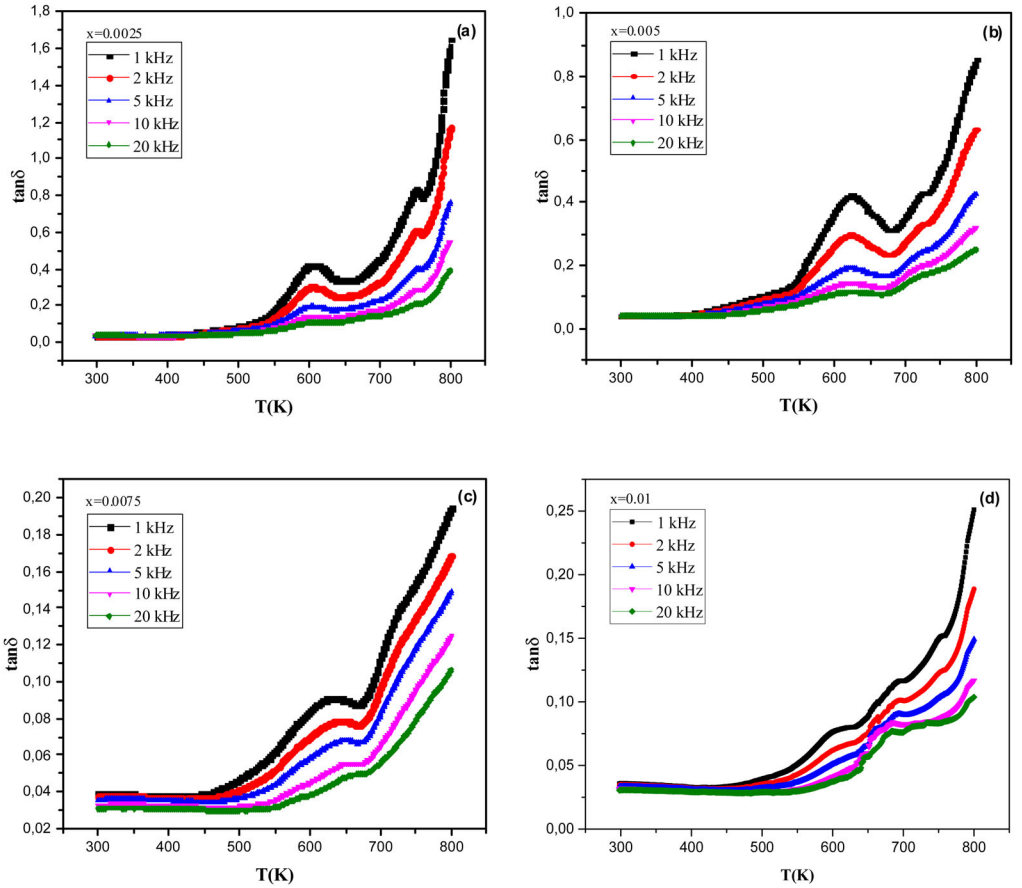

Figure 5. Variation of dielectric loss of (1-*x*)Pb($Zr_{0.50}$ $Ti_{0.50}$)O_3–xBa($W_{2/3}$ $Mn_{1/3}$)O_3 ((a) $x = 0.0025$, (b) $x = 0.005$, (c) $x = 0.0075$, and (d) $x = 0.01$) ceramics at selected frequencies as a function of temperature.

Table 1. Dielectric properties of (1–*x*)PZT–*x*BWM ceramics (at 1 kHz).

		Dielectric properties (at 298 K)		Dielectric properties (at T_C)	
Systeme	T_C (K)	ε_r	Tanδ	ε_{max}	tanδ
0.0025	664	1532	0.0343	13256	0.3389
0.005	690	1376	0.0338	13271	0.3213
0.0075	687	1248	0.0386	9472	0.0977
0.01	662	1401	0.0355	9430	0.099

(1–*x*)PZT–xBWM as a function of temperature at selected frequencies has exhibited that maximum or peak dielectric constant, tangent loss, and transition temperature are strongly dependent on x content in PZT–BWM.

References

[1] R. A. Pferner, G. Thurn, and F. Aldinger, Mechanical properties of PZT ceramics with tailored microstructure, *Mater. Chem. Phys.* **61** (1), 24 (1999). DOI: 10.1016/S0254-0584(99)00108-X.

[2] A. H. Macias *et al.*, Indentation size effect in soft PZT ceramics with tetragonal structure close to the MPB, *J. Phys. D: Appl. Phys.* **41** (3), 035407 (2008). DOI: 10.1088/0022-3727/41/3/035407.
[3] Z. He, and J. Ma, Constitutive modeling of the densification of PZT ceramics, *J. Phys. Chem. Solids* **64** (2), 177 (2003). DOI: 10.1016/S0022-3697(02)00170-1.
[4] S. K. Korchagina *et al.*, Rare-earth-doped $PbTiO_3$–$PbZrO_3$ solid solutions, *Inorg. Mater.* **45** (3), 287 (2009). DOI: 10.1134/S0020168509030133.
[5] M. R. Soares, A. M. R. Senos, and P. Q. Mantas, Phase coexistence region and dielectric properties of PZT ceramics, *J. Eur. Ceram. Soc.* **20** (3), 321 (2000). DOI: 10.1016/S0955-2219(99)00170-3.
[6] R. Yimnirun *et al.*, Stress-dependent scaling behavior of dynamic hysteresis in bulk soft ferroelectric ceramic, *Appl. Phys. Lett.* **89** (24), 242901 (2006). DOI: 10.1063/1.2403182.
[7] N. Setter, and E. L. Colla, *Ferroelectric Ceramics: Tutorial Review, Theory, Processing and Applications* (Birkhäuser, Basel, Boston, 1993).
[8] M. A. Mohiddon, A. Kumar, and K. L. Yadav, Effect of Nd doping on structural, dielectric and thermodynamic properties of PZT (65/35) ceramic, *Phys. B: Condens. Matter* **395** (1–2), 1 (2007). DOI: 10.1016/j.physb.2006.09.022.
[9] B. Jaffe, R. C. Williams, and, and H. Jaffe, *Piezoelectric Ceramics* (Academic Press, London, New York, 1971).
[10] A. Kumar, and S. K. Mishra, Dielectric, piezoelectric, and ferroelectric properties of lanthanum-modified PZTFN ceramics, *Int. J. Miner. Metall. Matt.* **21** (10), 1019 (2014). DOI: 10.1007/s12613-014-1003-9.
[11] V. Tiwari, and G. Srivastavan, The effect of Li_2CO_3 addition on the structural, dielectric and piezoelectric properties of PZT ceramics, *Ceram. Int.* **41** (2), 2774 (2015). DOI: 10.1016/j.ceramint.2014.10.096.
[12] C. C. Tsai *et al.*, The phase structure, electrical properties, and correlated characterizations of (Mn,Sb) co-tuned PZMnNS–PZT ceramics with relaxation behavior near the morphotropic phase boundary, *Ceram. Int.* **40** (8), 11713 (2014). DOI: 10.1016/j.ceramint.2014.03.185.
[13] G. Srivastava, A. Goswami, and A. M. Umarji, Temperature dependent structural and dielectric investigations of $PbZr_{0.5}Ti_{0.5}O_3$ solid solution at the morphotropic phase boundary, *Ceram. Int.* **39** (2), 1977 (2013). DOI: 10.1016/j.ceramint.2012.08.049.
[14] Ragini, R. R. *et al.*, Room temperature structure of $Pb(Zr_xTi_{1-x})O_3$ around the morphotropic phase boundary region: a Rietveld study, *J. Appl. Phys.* **92** (6), 3266 (2002). DOI: 10.1063/1.1483921.
[15] C. A. Oliveira *et al.*, Synthesis and characterization of lead zirconate titanate (PZT) obtained by two chemical methods, *Ceram. Int.* **40** (1), 1717 (2014). DOI: 10.1016/j.ceramint.2013.07.068.
[16] M. Valant *et al.*, A mechanism for low-temperature sintering, *J. Eur. Ceram. Soc.* **26** (13), 2777 (2006). DOI: 10.1016/j.jeurceramsoc.2005.06.026.
[17] N. Sahu, S. Panigrahi, and M. Kar, Structural investigation and dielectric studies on Mn substituted $Pb(Zr_{0.65}Ti_{0.35})O_3$ perovskite ceramics, *Ceram. Int.* **38** (2), 1549 (2012). DOI: 10.1016/j.ceramint.2011.09.040.
[18] B. Tiwari, and R. N. P. Choudhary, Frequency–temperature response of $Pb(Zr_{0.65-x}Ce_xTi_{0.35})O_3$ ferroelectric ceramics: structural and dielectric studies, *Phys. B: Condens. Matt.* **404** (21), 4111 (2009). DOI: 10.1016/j.physb.2009.07.171.
[19] R. Ranjan, R. Kumar, and R. N. P. Choudhary, Effect of Sm substitution on structural, dielectric, and transport properties of PZT ceramics, *Resea. Lette. Phys.* **382578** (2009) (2009). DOI: 10.1155/2009/382578.
[20] Z. Liu *et al.*, Synthesis, structure, and properties of the $PbZrO_3$-$PbTiO_3$-$Bi(Zn_{2/3}Nb_{1/3})O_3$ ternary solid solution system around the morphotropic phase boundary, *Phys. Status Solidi A.* **215** (20), 1 (2018). DOI: 10.1002/pssa.201701007.
[21] Y. Xu, *Ferroelectrics Materials and Their Applications* (North Holland, Amsterdam, 1991).

[22] P. Singh *et al.*, Effect of Samarium substitution on dielectric properties of (Pb)(Zr, Ti, Fe, Nb)O_3 type ceramic system, *Ceram. Int.* **35** (8), 3335 (2009). DOI: 10.1016/j.ceramint.2009.05.036.

[23] B. Behera, P. Nayak, and R. N. P. Choudhary, Structural and electrical properties of $LiBa_2V_5O_{15}$ ceramics, *Phys. Stat. Sol. (A)* **204** (7), 2479 (2007). DOI: 10.1002/pssa.200622592.

[24] S. R. Shannigrahi *et al.*, Effect of rare earth (La, Nd, Sm, Eu, Gd, Dy, Er and Yb) ion substitutions on the microstructural and electrical properties of sol-gel grown PZT ceramics, *J. Eur. Ceram. Soc.* **24** (1), 163 (2004). DOI: 10.1016/S0955-2219(03)00316-9.

[25] M. E. Lines, and, and A. M. Glass, *Principles and Applications of Ferroelectrics and Related Materials* (Oxford University Press, London, 1977).

[26] O. P. Thakur, and C. Prakash, Dielectric properties of samarium substituted barium strontium titanate, *Phase. Trans.* **76** (6), 567 (2003). DOI: 10.1080/01411590290030708.

[27] R. P. Tandon *et al.*, The effect of neodymium oxide on dielectric and electromechanical properties of lead zirconate titanate ceramics, *Mater. Lett.* **20** (3–4), 165 (1994). DOI: 10.1016/0167-577X(94)90081-7.